

Report Number 10/05

Ergodic directional switching in mobile insect groups

by

**Carlos Escudero, Christian A. Yates, Jerome Buhl, Iain D. Couzin,
Radek Erban, Ioannis G. Kevrekidis, and Philip K. Maini**



Oxford Centre for Collaborative Applied Mathematics
Mathematical Institute
24 - 29 St Giles'
Oxford
OX1 3LB
England

Ergodic directional switching in mobile insect groups

Carlos Escudero¹, Christian A. Yates², Jerome Buhl³, Iain D. Couzin⁴,

Radek Erban^{2,5}, Ioannis G. Kevrekidis⁴, and Philip K. Maini^{2,6}

¹ ICMAT (CSIC-UAM-UC3M-UCM),

Universidad Autónoma de Madrid, 28049 Madrid, Spain

² Centre for Mathematical Biology,

Mathematical Institute, University of Oxford,

24-29 St. Giles', Oxford, OX1 3LB, United Kingdom

³ The University of Sydney, NSW, Australia

⁴ Department of Chemical Engineering,

Program in Applied and Computational Mathematics and Mathematics,

Princeton University, Princeton, NJ 08544, USA

⁵ Oxford Centre for Collaborative Applied Mathematics,

Mathematical Institute, University of Oxford,

24-29 St. Giles', Oxford, OX1 3LB, United Kingdom

⁶ Department of Biochemistry,

Oxford Centre for Integrative Systems Biology,

University of Oxford, South Parks Road,

Oxford OX1 3QU, United Kingdom

We obtain a Fokker-Planck equation describing experimental data on the collective motion of locusts. The noise is of internal origin and due to the discrete character and finite number of constituents. The stationary probability distribution shows a rich phenomenology including the non-monotonic behavior of several order/disorder transition indicators in noise intensity. This complex behavior arises as the system's response to the amount of randomness in it. Its counterintuitive character challenges the standard interpretation of noise induced transitions and calls for an extension of its phenomenology in order to include certain classes of biologically motivated models. Our results suggest that the collective switches of the group's direction of motion might be due to a random ergodic effect and as such they are inherent to group formation.

PACS numbers: 87.23.Cc, 05.40.-a, 05.65.+b, 87.10.Mn

Emergence can be defined as the appearance of rich structures on a large scale resulting from a multiplicity of simple interactions at a considerably smaller scale. Collective animal motion is a paradigmatic example of such an emergent phenomenon. Depending on the species, there may exist different hierarchical levels that determine how collective displacements are realized. For example, in primate groups, an individual's dominance status can affect its role in initializing collective movement. In the case of swarming locusts no such hierarchies are present; the ability of each individual to guide the band appears to be distributed relatively evenly throughout the insect group. Herein we will concentrate on groups of wingless locust nymphs which form marching bands rather than flying swarms [1]. The onset of collective motion in locusts was experimentally demonstrated in [1], where it was shown that sufficiently large insect densities placed in a ring-shaped arena gave rise to a coherent displacement of the band. Low densities were characterized by random dispersal of the individuals, while for intermediate densities the coherent motion was interrupted by sudden changes of direction (hereafter referred to as “switches”). This phenomenology was partially rationalized by means of an adapted model based on that of Czirik *et al.* [2], who formulate a paradigmatic model for collective animal behavior in one dimension. In their original model the position, x_i , and velocity, u_i , of locust i are evolved using the following two rules, identical for each individual, $i = 1, \dots, N$,

$$x_i(t+1) = x_i(t) + v_0 u_i(t),$$

$$u_i(t+1) = G(\bar{u}_i) + \xi_i,$$

where N is the total number of locusts. Here \bar{u}_i is the mean of the nondimensionalised velocities of locusts within a certain radius, R , of the position, x_i , of locust i . The function G is such that $G(u) = (1 + K)^{-1}[u + K \operatorname{sgn}(u)]$ for a positive constant K , where $\operatorname{sgn}(u)$ denotes the sign of u . The role of G is to adjust the average nondimensionalised velocity perceived by each particle towards unity. v_0 is a constant associated with the chosen time scale and ξ_i is a random number drawn from the uniform distribution in $[-\eta/2, \eta/2]$. The adapted version of the model used in [1] to model the movements of locust nymphs in a quasi-one-dimensional arena takes the form

$$\frac{dx_i}{dt} = u_i, \quad du_i = [G(\bar{u}_i) - u_i]dt + \beta_1 dW_i, \quad \text{for } i = 1, \dots, N, \quad (1)$$

where dW_i denotes the increments of independent Wiener processes, β_1 is a positive constant describing the amplitude of the noise and the function G is as above.

A biologically motivated refinement of the model described by Eq. (1) was given in [3], where it was demonstrated that individual locusts increase the randomness of their movements in response to a loss of group alignment. This behavior is the result of a particular multiplicative form of the noise term (see Eq. (2)), as opposed to the additive noise in Eq. (1); this characteristic was shown to increase the coherence of the group motion and to reduce the frequency of direction switches [3]. The key point in the analysis performed in [3] was the estimation of coefficients of an effective Fokker-Planck equation (FPE) [4], which is written in terms of a macroscopic (low-dimensional) observable [5], the average velocity of the marching group, derived directly from the experimental data. In the present work we approximate the drift and diffusion coefficients of the effective FPE by analytical functions. This permits a more thorough analysis and fosters further understanding of collective dynamics of locusts. In addition we compare our results with those of Eq. (1), and discuss the disparities between the two models.

The model. Coarse-grained analysis [4] allows us to obtain an effective FPE describing the collective behavior of the locusts at the macroscopic level. By using this coarse-graining technique (see [3]) we were able to extract the coefficients of the assumed underlying FPE describing the alignment of the locusts from the experimental data presented in [1]. This approach enables us to reduce our system - comprising a large number of degrees of freedom - to a single collective variable, u , (referred to variably, hereafter, as ‘alignment’ or ‘average velocity’) which describes the system’s macroscopic behavior. The derived FPE has a simple form and it can be expressed as

$$\partial_t P = -\alpha_2 \partial_u \left[\left(u - \frac{u^3}{1-u^2} \right) P \right] + \frac{\beta_2}{N} \partial_{uu} [(1-u^2)P], \quad (2)$$

for the probability $P(u, t)du dt$ of finding the system with an average velocity in the interval $(u, u + du)$ during the time interval $(t, t + dt)$; note that the experimental situation in [1] is quasi-one-dimensional, allowing the use of a one-dimensional FPE [3].

The derived FPE (2) describing the alignment is a reasonably accurate approximation to the unknown FPE assumed to underly the motion of the locusts, which captures their experimental swarming behavior. It should be noted that this technique is only appropriate if the system being studied is amenable to this sort of reduction.

For asymptotically large values of N , α_2^{-1} (in equation (2)) denotes the order of magnitude of the relaxation time characterizing how long it takes the entire group to become ordered when starting from a disordered configuration, and $N\beta_2^{-1}$ indicates the order of magnitude of the characteristic time over which the fluctuations of the mean velocity develop. For the range of experimentally considered locust numbers ($5 \leq N \leq 40$) the derived values of α_2 and β_2 are approximately constant while we expect the presence of a boundary layer for smaller values of N . Since our results in [3] are rather noisy our goal is to fit the order of magnitude of the model parameters instead of attempting to obtain precise estimates. Comparing the proposed analytical coefficients of Eq. (2) to those derived in [3], from the experimental data in [1], we obtain $\beta_2/\alpha_2 = 2.4 \pm 1.7$. Employing the mean switching time measurements in [3] we find $\alpha_2 = (6.65 \pm 2.63)10^{-4} s^{-1}$ and $\beta_2 = (1.62 \pm 0.52)10^{-3} s^{-1}$.

The FPE corresponding to Eq. (1) can be obtained as a mean-field approximation,

$$\partial_t P = -\alpha_1 \partial_u \{[\text{sgn}(u) - u]P\} + \frac{\beta_1}{N} \partial_{uu} P, \quad (3)$$

where $\alpha_1 = K/(1+K)$ and K is defined as for the function G in Eq. (1). The stationary solution of the FPE (3) can be derived as follows:

$$P_s(u) = \frac{\sqrt{\frac{\alpha_1 N}{2\pi\beta_1}} \exp\left(-\frac{\alpha_1 N}{2\beta_1}\right)}{1 + \text{erf}\left(\sqrt{\frac{\alpha_1 N}{2\beta_1}}\right)} \exp\left[\frac{\alpha_1 N}{\beta_1} \left(|u| - \frac{1}{2}u^2\right)\right]. \quad (4)$$

The maxima of this stationary probability distribution (SPD) stay constant for all parameter values. A straightforward inspection of this formula reveals that values of the two maxima $u_{\max} = \pm 1$ and the minimum $u_{\min} = 0$ are independent of the parameter values.

In the absence of sources and sinks of probability, we can also derive the SPD of the experimentally motivated FPE (2):

$$P_s(u) = \mathcal{N}(1-u^2)^{-1-N\alpha_2/\beta_2} \exp\left[-\frac{N\alpha_2/(2\beta_2)}{1-u^2}\right], \quad (5)$$

where $\mathcal{N}^{-1} = \int_{-1}^1 (1 - u^2)^{-1-N\alpha_2/\beta_2} \exp[-N\alpha_2/[2\beta_2(1 - u^2)]] du$ is the inverse of the normalization constant. This SPD is bounded, compactly supported in $[-1, 1]$ and bimodal for all values of the parameters.

Noise induced transitions have been studied traditionally by means of the dynamics of the extrema of the SPD [6]. For the biologically motivated FPE (2) the SPD shows one minimum always located at $u_{\min} = 0$, and two maxima at $u_{\max} = \pm\sqrt{\alpha_2 + 2\beta_2/N}/\sqrt{2\alpha_2 + 2\beta_2/N}$, which exist for all parameter values. One immediately notes $|u_{\max}| \in (1/\sqrt{2}, 1)$, a fact related to the shape of the “deterministic potential” (the potential in the absence of noise), which is the negative integral of the drift coefficient,

$$\mathcal{V}(u) = -\int_0^u \alpha_2 \left(s - \frac{s^3}{1 - s^2} \right) ds = -\alpha_2 \left[u^2 + \frac{1}{2} \ln(1 - u^2) \right]. \quad (6)$$

This potential is bistable with one maximum located at the origin and two minima at $\pm 1/\sqrt{2}$ independent of the parameter values. For increasing noise intensity the probability maxima of the SPD (5) (corresponding to the biologically motivated FPE (2)) separate from the deterministic potential minima $\pm 1/\sqrt{2}$ and approach the boundary points ± 1 . These facets of the SPD, when considered in the context of the classical theory of noise induced transitions, imply that the system is becoming ordered [6]: the SPD maxima, representing the states in which the system will most likely be found, are further apart and thus there is a clearer differentiation among those states. However, the experimental evidence, based on switching times which decrease as the noise magnitude increases, reveals that the system becomes disordered [1]. This indicates that for complex systems the reduction of the dynamics to the evolution of the extrema might not be adequate in some experimentally motivated situations.

Barrier Height. Another indicator of order/disorder is the barrier height of the effective potential. For the model given by Eq. (1) the barrier height decreases monotonically as the noise intensity increases as can be seen from Eq. (7)

$$\mathcal{V}_{\text{eff}}(u) = -\frac{\alpha_1 N}{\beta_1} \left(|u| - \frac{1}{2} u^2 \right), \quad \Delta \mathcal{V}_{\text{eff}} \equiv \mathcal{V}_{\text{eff}}(u_{\min}) - \mathcal{V}_{\text{eff}}(u_{\max}) = \frac{\alpha_1 N}{2\beta_1}, \quad (7)$$

where \mathcal{V}_{eff} is the effective potential and $\Delta \mathcal{V}_{\text{eff}}$ the corresponding barrier height.

The effective potential for our revised model (Eq. (2)) is given as

$$\mathcal{V}_{\text{eff}}(u) \equiv -\ln[P_s(u)] = \frac{N\alpha_2}{2\beta_2(1 - u^2)} + \left(1 + \frac{N\alpha_2}{2\beta_2} \right) \ln(1 - u^2), \quad (8)$$

and the corresponding barrier height is

$$\Delta \mathcal{V}_{\text{eff}} \equiv \mathcal{V}_{\text{eff}}(u_{\min}) - \mathcal{V}_{\text{eff}}(u_{\max}) = -1 - \frac{N\alpha_2}{2\beta_2} + \left(1 + \frac{N\alpha_2}{\beta_2} \right) \ln \left(2 + \frac{2\beta_2}{N\alpha_2} \right). \quad (9)$$

As a function of noise intensity the barrier height presents a minimum at $[\beta_2/(N\alpha_2)]_{\min} \approx 0.76$. This means that for $\beta_2/(N\alpha_2) < [\beta_2/(N\alpha_2)]_{\min}$ (sub-threshold) the barrier height diminishes for stronger noise, but for $\beta_2/(N\alpha_2) > [\beta_2/(N\alpha_2)]_{\min}$ (super-threshold) it increases as the noise strength grows. Indeed, $\Delta \mathcal{V}_{\text{eff}} \approx [\ln(2) - 1/2](N\alpha_2/\beta_2)$ when $N\alpha_2/\beta_2 \rightarrow \infty$ and $\Delta \mathcal{V}_{\text{eff}} \approx -\ln(N\alpha_2/\beta_2)$ when $N\alpha_2/\beta_2 \rightarrow 0$. This suggests that, while increased noise causes the system to become more disordered for sub-threshold noise intensities, super-threshold intensities might cause the system to become more ordered as the noise grows. In short, the ‘barrier height’ order parameter shows a clear non-monotonicity when considered as a function of noise strength. This looks like a counterintuitive reentrant behavior where the noise can have an ordering effect for supercritical intensities [6]. Although this behavior is interesting in itself, it is not biologically relevant, as it requires a number of individuals $N \approx 3$ beyond the model validity. Both characteristics of the SPD (5) of our refined model, displacement of the location of the maxima and non-monotonic variation of the barrier height, can be seen in Fig. 1 (a)-(b).

Mean Switching Time. We can further explore the model properties by considering the mean switching time, $T(u)$, defined as the first time, on average, that the alignment of the system, u , initialized such that $-1 < u < 0$, reaches the origin ($u = 0$). For our revised model the moments of the switching time distribution are given, recursively, by the solution of the equation

$$\alpha_2 \left(u - \frac{u^3}{1 - u^2} \right) \partial_u T_n + \frac{\beta_2}{N} (1 - u^2) \partial_{uu} T_n = -n T_{n-1}, \quad (10)$$

where T_n is the n^{th} moment, correspondingly, $T \equiv T_1$ is the mean switching time and $T_0 \equiv 1$. The boundary conditions $T(0) = 0$ and $T'(-1) = 0$ represent zero probability flux through $u = -1$. Eq. (10) is directly derived from

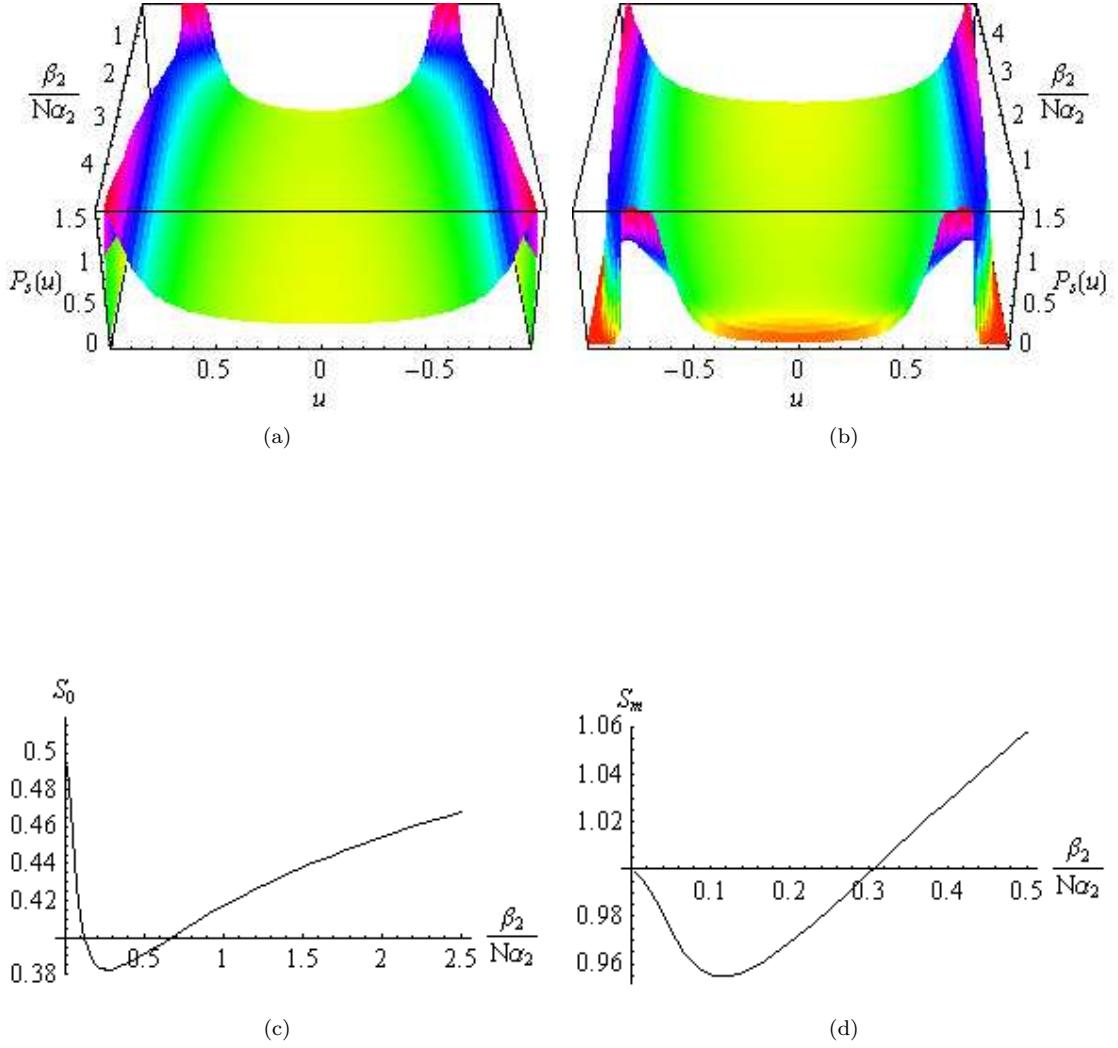


FIG. 1: Panels (a) and (b) show the profile of the SPD, $P_s(u)$, from Eq. (5) plotted against the normalized mean velocity u for a varying noise intensity $\beta_2/(N\alpha_2)$ from two angles. Panel (c) displays the second moment of the revised model, centered at the origin, S_0 , versus noise strength $\beta_2/(N\alpha_2)$ and panel (d) shows the second moment at a maximum, S_m , versus noise strength $\beta_2/(N\alpha_2)$. The minima are attained for $\beta_2/(N\alpha_2) \approx 0.27$ (S_0) and for $\beta_2/(N\alpha_2) \approx 0.12$ (S_m).

the FPE using methods from [7]. The solution to this equation for $n = 1$ is

$$T(u) = \frac{N}{\beta_2} \int_u^0 \exp \left[\frac{N\alpha_2/(2\beta_2)}{1-v^2} \right] (1-v^2)^{N\alpha_2/\beta_2} \int_{-1}^v \exp \left[-\frac{N\alpha_2/(2\beta_2)}{1-w^2} \right] (1-w^2)^{-1-N\alpha_2/\beta_2} dw dv.$$

This expression appears complicated, but one can derive its asymptotic expansion for large values of $N\alpha_2/\beta_2$ (which implies large N as α_2 and β_2 are approximately constant). It has the simple form $T(-1/\sqrt{2}) \approx \frac{\sqrt{2}\pi}{\alpha_2} \left(\frac{2}{\sqrt{e}} \right)^{N\alpha_2/\beta_2}$, which reveals a pure exponential growth in the inverse noise intensity $N\alpha_2/\beta_2$ for asymptotically large values. Further moments of the switching time distribution can be calculated from Eq. (10) for $n > 1$. In the limit $N \rightarrow \infty$ one finds the relation $T_n = n!T^n$. This relationship implies in turn that the switching process is a Poisson process.

We can also compute the first passage time for the model Eq. (1). In this case we solve the equation $\alpha_1[\text{sgn}(u) - u]\partial_u T + \frac{\beta_1}{N}\partial_{uu}T = -1$, subject to the boundary conditions $T(0) = 0$ and $T'(-\infty) = 0$, where the latter condition is

the analogue of the previous zero flux condition adapted for an SPD with infinite support. We find

$$T(u) = \sqrt{\frac{\pi N}{2\alpha_1\beta_1}} \int_u^0 \exp\left[\frac{N\alpha_1}{2\beta_1}(1+v)^2\right] \left\{2 - \operatorname{erfc}\left[\sqrt{\frac{\alpha_1 N}{2\beta_1}}(1+v)\right]\right\} dv,$$

which also behaves exponentially in N for large values of N but this time with an N dependent prefactor (see Supplementary Information of [3]). The relation between these two mean switching times (the model Eq. (1) and that of the revised model [3]) is extensively discussed in [3], so we will not reproduce the discussion here.

Now we compare the theoretical results with the exponential fitting we have performed on experimental data from [1] for both the first and second moments of the switching time distribution. The data is insufficient for us to reliably obtain any moments higher than the second. For the mean switching time T and second moment T_2 we found

$$T = (970 \pm 120) \exp[(0.045 \pm 0.007)N] \text{ s}, \quad \sqrt{T_2/2} = (1300 \pm 190) \exp[(0.041 \pm 0.008)N] \text{ s}.$$

According to the relation $T_n = n!T^n$, for the moments of the exponential distribution, these two values should be the same if the switching process were Poisson. Note that the exponential growth is the same for both (within errors), while the prefactor is larger for the second moment. This suggests that the switching process is Poisson for large N , that is, the probability distribution for the switching events is $\mathcal{P} = T^{-1} \exp(-t/T)$. For small values of N the behavior is more stochastic, as signalled by the larger prefactor of the second moment (when N is small the prefactor dominates over the exponential). If the switching process is Poisson this has a series of consequences concerning predictability: the standard deviation being equal to the mean implies a 100% error in predictions. Furthermore, switching events are uncorrelated, the most probable time for switching is $t = 0$, and the distribution tail falls off exponentially for long times. This allows for a higher probability of rare events than would be allowed by a Gaussian tail. All these factors imply that switching events are almost unpredictable from a practical viewpoint. This also implies that the switching process is Markovian, as predicted by the FPE. This can be seen from the double-welled FPE (2) in the large N limit. After a short time the system relaxes to one potential minimum where it stays an exponentially long time until the switch happens. Since practically all switches start at the minimum this erases the memory and the Markov property is recovered. The verification of this theoretical prediction with the experimental data suggests that no important correlations have been suppressed in the coarse-grained computation in [3], and that this method, and the FPE (2), are suitable to describe the locust dynamics exhibited by the experimental data.

Second Moments. Another indicator of the stochastic properties of the system is the second moment. The second moment measures the spread of the mean velocity, u , with respect to some reference value. We consider two variants, one centered at the origin $S_0 \equiv \int_{-1}^1 u^2 P_s(u) du$, and one centered at one of the maxima of the probability distribution $S_m \equiv \int_{-1}^1 (u - u_{\max})^2 P_s(u) du$. Of course, the value of S_m is the same for both maxima as a consequence of the symmetry of the system. These integrals have been computed numerically and are represented in Fig. 1(c), centered at the origin, and 1(d) centered at a maximum. Both show non-monotonic behavior in noise intensity, but attain their minima for different values of the noise amplitude. This non-monotonic behavior, as well as the behavior of the effective barrier height, are not reflected in the relationship between mean switching time and the size of the noise parameter ($N\alpha_2/\beta_2$): the mean switching time grows monotonically with noise amplitude. For comparison we note that both moments S_0 and S_m grow monotonically with the inverse noise intensity in the model given by Eq. (1); in this case they are

$$S_0 = 1 + \frac{\beta_1}{\alpha_1 N} + \frac{\sqrt{\frac{2\beta_1}{\pi\alpha_1 N}} \exp\left(-\frac{\alpha_1 N}{2\beta_1}\right)}{1 + \operatorname{erf}\left(\sqrt{\frac{\alpha_1 N}{2\beta_1}}\right)}, \quad S_m = 2 + \frac{\beta_1}{\alpha_1 N} + \frac{\sqrt{\frac{2\beta_1}{\pi\alpha_1 N}} \exp\left(-\frac{\alpha_1 N}{2\beta_1}\right)}{1 + \operatorname{erf}\left(\sqrt{\frac{\alpha_1 N}{2\beta_1}}\right)}. \quad (11)$$

There is another feature of the second moments of the revised model [3], other than the non-monotonic behavior, that reveals new characteristics of the collective motion of locusts not reflected by the model Eq. (1). In this model a reduction in the number of individuals increases the values of both second moments. In the stronger-noise situation the probability distribution tails grow, which implies that there are more individuals with a higher (absolute value) velocity. In our case the probability is compactly supported in $[-1, 1]$, as a consequence of the biological fact that the propagation cannot be better than perfect. For realistic values of the parameters the system is in the weak noise regime (see Fig. 1(c)). This means that the second moment centered at the origin decreases for a decreasing number of locusts, exactly the opposite trend to that of the model Eq. (1). The reason is that the probability of finding the system in the neighborhood of $u = 0$ grows considerably for stronger noise (as reflected by the decreasing barrier height), largely compensating for the drift of the maxima towards the boundaries of the support of the SPD. The

experimentally derived value of $\beta_2/N\alpha_2 = 0.12 \pm 0.08$ for $N = 20$ agrees with the minimizing value of the second moment centered at a maximum, $\beta_2/N\alpha_2 \approx 0.12$ (see Fig. 1(d)). This implies that its behavior is not very sensitive to small changes in the number of locusts.

Conclusions. We have seen that the FPE derived from the coarse-grained analysis of experimental data on the movement of locusts shows an interesting phenomenology. Different indicators of order/disorder may vary non-monotonically with noise intensity, possibly in a contradictory manner. These findings reveal that these indicators might not be suitable for the biologically motivated models studied in this paper. We have also shown that the direction switches are independently distributed for large numbers of individuals. This makes them almost unpredictable from a practical viewpoint. It seems that directional switches are produced by an accumulation of errors (made by the locusts when trying to adapt their velocity to that of their neighbors) that ordinarily interfere and cancel each other out but, for exponentially long times, have the possibility of accumulating and producing a switch. According to the results presented here, specifically the finding of the Poissonian character of the switching events, it seems possible that directional switches are produced as a consequence of the ergodic random evolution of the system. We note the similarity of this process with Ising model ergodic magnetization changes [8]. Indeed, the model of Eq. (1) can be thought of as an Ising model with moving spins. It seems that the ergodic nature of the finite size Ising model is preserved despite introducing movement of the spins. More importantly it seems that this is a plausible explanation, in the absence of external stimuli, of the sudden changes of direction observed in animal groups.

Acknowledgements. The authors are grateful to David Sumpter for useful comments and discussions. This work was supported by the Oxford-Princeton Research Partnership grant. CE acknowledges support by the MICINN (Spain) through Project No. MTM2008-03754. CAY thanks EPSRC for funding via the Systems Biology Doctoral Training Centre, University of Oxford. This publication is based on work (R.E.) supported by Award No. KUK-C1- 013-04, made by the King Abdullah University of Science and Technology (KAUST); RE also thanks Somerville College, Oxford for Fulford Junior Research Fellowship. PKM was partially supported by a Royal Society Wolfson Research Merit Award.

-
- [1] J. Buhl *et al.*, Science **312**, 1402 (2006).
 - [2] A. Czirók *et al.*, Phys. Rev. Lett. **82**, 209 (1999).
 - [3] C. Yates *et al.*, Proc. Natl. Acad. Sci. USA **106**, 5464 (2009).
 - [4] R. Erban *et al.*, J. Chem. Phys. **124**, 084106 (2006).
 - [5] R. Erban *et al.*, J. Chem. Phys. **126**, 155103 (2007).
 - [6] W. Horsthemke and R. Lefever, *Noise-Induced Transitions* (Springer-Verlag, Berlin, 1984).
 - [7] C. W. Gardiner, *Handbook of Stochastic Methods* (Springer-Verlag, Berlin, 1996).
 - [8] K. Brendel *et al.*, Phys. Rev. E **67**, 026119 (2003).

RECENT REPORTS

29/09	All-at-once preconditioning in PDE-constrained optimization	Rees Stoll Wathen
30/09	An hp-Local Discontinuous Galerkin method for Parabolic Integro-Differential Equations	Pani Yadav
31/09	Stochastic neural field theory and the system-size expansion	Bressloff
32/09	A Hamiltonian Krylov-Schur-type method based on the symplectic Lanczos process	Benner Faßbender Stoll
33/09	Nematic liquid crystals : from Maier-Saupe to a continuum theory	Ball Majumdar
34/09	Tangent unit-vector fields: nonabelian homotopy invariants and the Dirichlet energy	Majumdar Robbins Zyskin
35/09	A metabolite-sensitive, thermodynamically-constrained model of cardiac cross-bridge cycling: Implications for force development during ischemia	Tran Smith Loiselle Crampin
36/09	Modelling bacterial behaviour close to a no-slip plane boundary: the influence of bacterial geometry	Shum Gaffney Smith
37/09	Optimal L2-error estimates for the semidiscrete Galerkin approximation to a second order linear parabolic initial and boundary value problem with nonsmooth initial data	Goswami Pani
38/09	Optimal L2 estimates for semidiscrete Galerkin methods for parabolic integro-differential equations with nonsmooth data	Goswami Pani Yadav
39/09	Spatially structured oscillations in a two-dimensional excitatory neuronal network with synaptic depression	Kilpatrick Bressloff
40/09	Stationary bumps in a piecewise smooth neural field model with synaptic depression	Kilpatrick Bressloff
41/09	Homogenization for advection-diffusion in a perforated domain	Haynes Hoang Norris Zygalakis
42/09	Fast stochastic simulation of biochemical reaction systems by alternative formulations of the Chemical Langevin Equation	Melykuti Burrage Zygalakis

43/09	Pseudoreplication invalidates the results of many neuroscientific studies	Lazic
44/09	Cardiac cell modelling: Observations from the heart of the cardiac physiome project	Finka <i>et al.</i>
45/09	A Hybrid Radial Basis Function - Pseudospectral Method for Thermal Convection in a 3-D Spherical Shell	Wright Flyer
46/09	Refining self-propelled particle models for collective behaviour	Yates Baker Erban Maini
47/09	Stochastic Partial Differential Equations as priors in ensemble methods for solving inverse problems	Potsepaev Farmer Aziz
48/09	DiffFUZZY: A fuzzy spectral clustering algorithm for complex data sets	Cominetti <i>et al.</i>
01/10	Fluctuations and instability in sedimentation	Guazzelli Hinch
02/10	Determining the equation of state of highly plasticised metals from boundary velocimetry	Hinch
03/10	Stability of bumps in piecewise smooth neural elds with nonlinear adaptation	Kilpatrick Bressloff
04/10	Random intermittent search and the tug-of-war model of motor-driven transport	Newby Bressloff

Copies of these, and any other OCCAM reports can be obtained from:

**Oxford Centre for Collaborative Applied Mathematics
Mathematical Institute
24 - 29 St Giles'
Oxford
OX1 3LB
England
www.maths.ox.ac.uk/occam**